High-Torque Density and Voltage Overmodulation for Five-Phase Induction Motor Drives

Luca Vancini, *Member, IEEE*, Michele Mengoni, *Member, IEEE*, Gabriele Rizzoli, Luca Zarri, *Senior Member, IEEE*, and Angelo Tani

***Abstract*—The torque density of a multiphase motor can be increased without exceeding the admissible current of the drive if the high-order spatial harmonics of the magnetic field in the air gap are appropriately synchronized with the fundamental one. Notably, due to the converter voltage limitation, this method is feasible only if the speed of the rotor is below its base speed. As the speed of the rotor increases, the voltage must correspondingly increase to sustain the field harmonics in the air gap. Above the base speed, the prevalent strategy in motor control focuses on regulating only the fundamental component of the magnetic field in the air gap. Nevertheless, this paper presents a new method that employs the injection of voltage harmonics to extend the linear modulation range of the fundamental voltage vector, thereby improving motor performance. In the field weakening region, an increase in the magnitude of the stator voltage vector improves the motor power and torque by over 40%. Experimental tests on a five-phase induction motor drive confirm the feasibility and the effectiveness of the developed control scheme. Overall, this approach shows great potential for improving motor performance and has applications in various sectors of motor control.**

***Index Terms*—Multiphase induction motor drives, overmodulation, variable speed drives.**

I. Introduction

MULTIPHASE drives, i.e., drives based on machines with more than three phases, are particularly suitable for high-reliability applications where fault tolerance is essential, such as vehicle and naval propulsion systems or more-electric aircrafts [1], [2]. Multiphase machines have a unique feature: the low-order spatial harmonics of the magnetic field in the air gap can be controlled independently, providing a significant advantage in the control quality. The independent control of the lower spatial harmonics of the magnetic field is possible because the number of degrees of freedom is higher than in traditional three-phase systems. This feature can be used to achieve better fault tolerance [3], [4], [5], [6], control multiple motors [7], [8], [9] and increase the motor torque density. Several papers have been published focusing on the low-speed range of induction motors [10], [11], [12], [13]. They consider the constraints resulting from the admissible current and the iron saturation of the machine because the design aspects of the electric machine and the power converter significantly impact the performance of the motor. The concept of a high-torque density motor is based on injecting a third-harmonic current component into the machine to enhance the fundamental harmonic component of the magnetic field in the air gap. Induction machines designed for this application usually have a non-distributed stator winding (one slot per pole per phase) to maximize the winding factor of the high-order field harmonic components [14]. During the design process, it is necessary to consider several electrical parameters, especially the iron losses and the magnetic saturation of the iron core, which could result in significant performance reduction.

The injection of a third-harmonic current can significantly enhance the machine torque density, making it particularly advantageous for applications in vehicle propulsion systems. The proposed solution capitalizes on the degrees of freedom offered by multiphase technology, aligning seamlessly with the demands for superior reliability and high torque density across diverse operating conditions, especially in typical traction applications [15], [16], [17].

When the machine works in the field weakening region, the injection of the third harmonic current is not applicable due to the limited dc link voltage [12]. When the inverter voltage constraint restricts the operating points of the motor, the inverter voltage must be used entirely to sustain the fundamental component of the currents. Enhancing the modulating index of the inverter proves to be more beneficial, effectively augmenting the available voltage of the machine.

In multiphase inverters, the linear modulation range can be extended by adequately managing the additional degrees of freedom of this technology [17]. In essence, the fundamental component of the voltage can be increased by injecting higher-order voltage harmonics with the proper magnitude and phase angle. This solution extends the maximum modulation index of

Manuscript received 27 December 2023; revised 26 February 2024; accepted 31 March 2024. Date of publication 7 May 2024; date of current version 22 July 2024. Paper 2023-IDC-1443.R1, presented at the 2022 IEEE Energy Conversion Congress and Exposition, 3, Nov. 30, and approved for publication in IEEE Transactions on Industry Applications by the Industrial Drives Committee of the IEEE Industry Applications Society DOI:[10.1109/ECCE50734.2022.9947419]. This work was supported in part by the National Recovery and Resilience Plan (NRRP), Mission 4 Component 2 Investment 1.3 - Call for tender No. 1561 of 11.10.2022 of Ministero dell'Università e della Ricerca (MUR), funded by the European Union – NextGenerationEU. Award Number: Project code PE0000021, Concession Decree No. 1561 of 11.10.2022 adopted by Ministero dell'Università e della Ricerca (MUR), CUP J33C22002890007. Project title: Network 4 Energy Sustainable Transition – NEST. *(Corresponding author: Luca Zarri.)*

The authors are with the Department of Electrical, Electronic and Information Engineering, University of Bologna, 40136 Bologna, Italy (e-mail: luca.vancini4@unibo.it; michele.mengoni@unibo.it; gabriele.rizzoli@unibo.it; luca.zarri2@unibo.it; angelo.tani@unibo.it).

Color versions of one or more figures in this article are available at https://doi.org/10.1109/TIA.2024.3397742.

Digital Object Identifier 10.1109/TIA.2024.3397742

the inverter but worsens the quality of the stator current and the stator Joule losses.

The motor torque can be increased by injecting current harmonics that shape the stator magnetic field at low speeds. Likewise, the injection of voltage harmonics can increase the maximum modulation index of the inverter at high speeds and the maximum torque in the field weakening region. Thus, high torque-density machines with the proposed control system can produce high torque at low speed by injecting a third harmonic current component into the stator windings; high efficiency at high speed can be achieved by increasing the maximum torque in the field weakening region.

This paper, which extends [19], aims to develop a robust control scheme for a high-torque density five-phase induction motor that maximizes its torque capability at all speeds rather than just at low regimes. The proposed control scheme can fully exploit the degrees of freedom of a multiphase system and improve the motor performance in different operating conditions, which is a significant advantage in various industrial applications.

Furthermore, the proposed control scheme can manage the transition between current injection in the low-speed region and voltage injection in the high-speed region. A theoretical analysis supports the developed solution, and the results of experimental tests confirm its feasibility. These results demonstrate the potential of the proposed solution in real-world scenarios.

The structure of the paper is as follows. Section II describes the mathematical model of a five-phase induction motor. Section III presents the strategy for increasing the torque density in the low-speed range. Section IV is dedicated to the description of the extended linear modulation region. Section V explains how the harmonic injection can improve motor performance in field weakening operation, while Section VI describes the control scheme of the five-phase induction motor drive. Section VII reports the experimental results obtained with a five-phase induction motor and a five-phase inverter.

II. Mathematical Model for Five-Phase Induction Machines With Concentrated Windings

According to the Vector Space Decomposition (VSD) [17], the model of a five-phase induction machine with concentrated windings (i.e., with one slot per pole per phase) can be represented by the following set of complex equations in the fundamental and the third harmonic subspaces:

$$\bar{v}_{S1} = R_S \bar{\imath}_{S1} + j\omega_1 \bar{\varphi}_{S1} + \frac{d\bar{\varphi}_{S1}}{dt} \tag{1}$$

$$0 = R_{R1}\bar{\imath}_{R1} + j\left(\omega_1 - \omega_m\right)\bar{\varphi}_{R1} + \frac{d\bar{\varphi}_{R1}}{dt} \tag{2}$$

$$\bar{\varphi}_{S1} = L_{S1}\bar{\imath}_{S1} + M_1\bar{\imath}_{R1} \tag{3}$$

$$\bar{\varphi}_{R1} = M_1\bar{\imath}_{S1} + L_{R1}\bar{\imath}_{R1} \tag{4}$$

$$\bar{v}_{S3} = R_S \bar{\imath}_{S3} + j\omega_3 \bar{\varphi}_{S3} + \frac{d\bar{\varphi}_{S3}}{dt} \tag{5}$$

$$0 = R_{R3}\bar{\imath}_{R3} + j\left(\omega_3 - 3\omega_m\right)\bar{\varphi}_{R3} + \frac{d\bar{\varphi}_{R3}}{dt} \tag{6}$$

$$\bar{\varphi}_{S3} = L_{S3}\bar{\imath}_{S3} + M_3\bar{\imath}_{R3} \tag{7}$$

$$\bar{\varphi}_{R3} = M_3\bar{\imath}_{S3} + L_{R3}\bar{\imath}_{R3} \tag{8}$$

$$T_1 = \frac{5}{2}p\,\bar{\imath}_{S1}\cdot j\bar{\varphi}_{S1} \tag{9}$$

$$T_3 = \frac{15}{2}p\,\bar{\imath}_{S3}\cdot j\bar{\varphi}_{S3} \tag{10}$$

where $\bar{v}_{S\rho}\,(\rho = 1,\ 3)$ are the space vectors of the stator voltages, $\bar{\imath}_{S\rho}$ and $\bar{\imath}_{R\rho}\,(\rho = 1,\ 3)$ are the space vectors of the stator and rotor currents, $\bar{\varphi}_{S\rho}$ and $\bar{\varphi}_{R\rho}\,(\rho = 1,\ 3)$ are the space vectors of the stator and rotor fluxes, ω_m is the electric angular speed of the rotor, p is the number of pole pairs, $R_{R\rho}$, $L_{S\rho}$, $L_{R\rho}$ and $M_\rho\,(\rho = 1,\ 3)$ are the rotor resistances, the self and mutual inductances of the stator and rotor windings. The stator resistance R_S is the same for all subspaces, $T_\rho\,(\rho = 1,\ 3)$ is the torque contribution of the ρth subspace, and the symbol "·" is the dot product between two space vectors, defined as the real part of the product of the first one times the complex conjugate of the second one. The sets of (1)–(4) and (5)–(8) are written respectively in the rotor-flux oriented reference frames $d_1 - q_1$ and $d_3 - q_3$ with electric angular speeds ω_1 and ω_3.

III. Control Strategy for High Torque Density in Constant Torque Region

The torque produced by the five-phase induction machine is the sum of the contributions generated in each subspace, i.e., $T = T_1 + T_3$. The torque density can be improved by controlling the third spatial harmonic of the air-gap magnetic field [10], [11]. If the third spatial harmonic of the magnetic field is synchronized with the fundamental component ($\omega_3 = 3\omega_1$), it is possible to properly align them. As a result, the waveform of the magnetic field in the air gap has a peak lower than the magnetic field produced by the fundamental component alone. The amplitude of the fundamental component can be increased without surpassing the rated peak value of the flux density or increasing the level of iron saturation [11]. If the leakage fluxes are neglected, the maximum value of the resulting magnetic field generated by the first and the third magnetic field can be expressed in terms of flux-producing currents i_{S1d} and i_{S3d} as follows [12]:

$$\max_{-\frac{\pi}{2}\leq\theta\leq\frac{\pi}{2}} \left\{ i_{S1d}\cos\left(\theta\right) - \frac{i_{S3d}}{3}\cos\left(3\theta\right) \right\} = i_{Sd,rated} \tag{11}$$

where $i_{Sd,rated}$ is the magnetizing current that produces the rated sinusoidal spatial distribution of the air-gap magnetic field, and $i_{S\rho d}$ and $i_{S\rho q}\,(\rho = 1,\ 3)$ are the $d - q$ components of the space vectors $\bar{\imath}_{S1}$ and $\bar{\imath}_{S3}$.

Maximizing the motor torque $T_1 + T_3$ resulting from (9)–(10) while the stator current and flux density are limited, is a non-trivial optimization problem, which involves a non-linear set of constraints. A simplified solution that does not need complicated calculations but valid only for machines with one slot per pole per phase is presented below [12]:

$$i_{S3d} \cong \frac{1}{2} i_{S1d} \tag{12}$$

$$i_{S3q} = 3\frac{\tau_{R3}}{\tau_{R1}}\frac{i_{S3d}}{i_{S1d}}i_{S1q} \tag{13}$$

where $\tau_{R\rho}$ $(\rho = 1,\ 3)$ are the rotor time constants defined as $\tau_{R\rho} = L_{R\rho}/R_{R\rho}$. Equations (12) and (13) show that, to increase the motor torque density, the stator currents of subspaces 1 and 3 can no longer be considered independent variables.

This method is suitable when the voltage required to inject $\bar{\imath}_{S1}$ and $\bar{\imath}_{S3}$ is lower than the available voltage. However, if the voltage constraint becomes the most binding, such as in the field weakening operation, the available voltage can only sustain the fundamental component of the field. In such a scenario, it is not possible to inject the harmonic current $\bar{\imath}_{S3}$.

IV. Extended Linear Modulation

According to the principles of the VSD, the modulating signals of a five-phase inverter depend on the voltage space vectors $\bar{v}_{S1}$ and $\bar{v}_{S3}$, and the zero-sequence component v_0, as follows:

$$m_k = \frac{1}{E_{DC}}\left(\bar{v}_{S1}\cdot\bar{\alpha}_k + \bar{v}_{S3}\cdot\bar{\alpha}_k^3 + v_0\right)\quad (k = 1,\ldots,5) \tag{14}$$

where E_{DC} is the DC-link voltage of the inverter, and $\bar{\alpha}_k = e^{j\frac{2}{5}\pi(k-1)}$. The modulating signals of (14) in the linear modulation region should satisfy the following constraints:

$$m_k \in [0, 1] \quad k = 1,\ldots,5. \tag{15}$$

In each switching period, the modulating signals can be ranked in ascending order (low, down, medium, up, high), denoted as L-D-M-U-H. Then, (15) implies the following inequality:

$$m_H - m_L \leq 1 \tag{16}$$

Inequality (16) combined with (14) can be rewritten in terms of voltage space vectors as follows:

$$\bar{m}_1\cdot\bar{A}_{1,HL} + \bar{m}_3\cdot\bar{A}_{3,HL} \leq 1 \tag{17}$$

where:

$$\bar{m}_\rho = \frac{\bar{v}_{S\rho}}{E_{DC}}\quad (\rho = 1,\ 3) \tag{18}$$

$$\bar{A}_{1,HL} = \bar{\alpha}_H - \bar{\alpha}_L,\ \ \bar{A}_{3,HL} = \bar{\alpha}_H^3 - \bar{\alpha}_L^3. \tag{19}$$

In the linear modulation region, $\bar{v}_{S3}$ could be set to zero or used for the current injection to maximize the electromagnetic torque (Fig. 1). When $\bar{v}_{S3}$ is set to zero, the maximum magnitude value of $\bar{v}_{S1}$ is equal to 0.526 E_{DC} [16].

For these reasons, the papers that illustrate the control systems for the high-torque density operation of multiphase drives usually focus only on the low-speed range, when the converter operates in the linear modulation region, without considering the other regions.

The overmodulation region for a multiphase inverter, unlike that for a three-phase inverter, involves an additional region called the extended linear region, located between the linear modulation region and the conventional overmodulation region, as shown in Fig. 1. The extended linear region does not have a counterpart in three-phase inverters. In this region, the converter can generate the reference voltage space vector $\bar{v}_{S1}$in the fundamental subspace only provided that proper voltage harmonics are injected into the other vector subspaces.

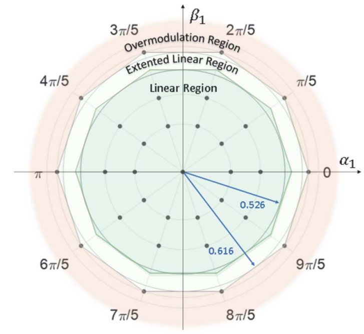

Fig. 1. Modulation regions of a five-phase inverter in the fundamental plane α_1-β_1.

In a five-phase motor drive, if the effect of the voltage harmonics in subspace $d_3 - q_3$ is tolerable (the stator inductance usually limits the additional current harmonics), the extended linear modulation can increase the magnitude of voltage by 17% [17], [18], [19], [20], [21].

V. Control Strategy for High Torque Density in the Field-Weakening Region

When the machine operates at high speeds, due to the voltage constraints of the inverter, it is no longer possible to inject the third-space current to increase the torque in the same way as in the constant torque region, and the machine must operate using only the fundamental component of the magnetic field. To maximize the torque, the fundamental component of the stator current must comply with the constraints resulting from the maximum inverter voltage, the maximum thermal current, and the breakdown torque, respectively represented by the following inequalities:

$$V_{S,\max}^2 \leq \omega_1^2 L_S^2\left[i_{S1d}^2 + \left(\sigma_1 i_{S1q}\right)^2\right] \tag{20}$$

$$I_{S1,\max}^2 \leq i_{S1d}^2 + i_{S1q}^2 \tag{21}$$

$$i_{S1d} \leq \sigma_1\ |i_{S1q}| \tag{22}$$

where $V_{S,\max}$ is the maximum admissible stator voltage. Equation (20) is obtained from (1)–(4) in steady-state conditions neglecting the resistive voltage drops. The maximum stator current is $I_{S,\max}$, and σ_1 is the leakage factor ($\sigma_1 = 1 - M_1^2/L_{S1}L_{R1}$). By combining (3), (4), (9), (20) and (21), it is possible to express the maximum value of torque T_1 as follows:

$$T_{\max} = \frac{5}{4}p\,\frac{1-\sigma_1}{\sigma_1}\frac{V_{S,\max}^2}{\omega_1 L_{S1}}. \tag{23}$$

Equation (23) shows that the maximum motor torque is determined by the available voltage squared, and even a slight increase in voltage can significantly boost the motor torque. Therefore, the motor performance strictly depends on $V_{S,\max}$ when the machine operates in the field-weakening region. In this

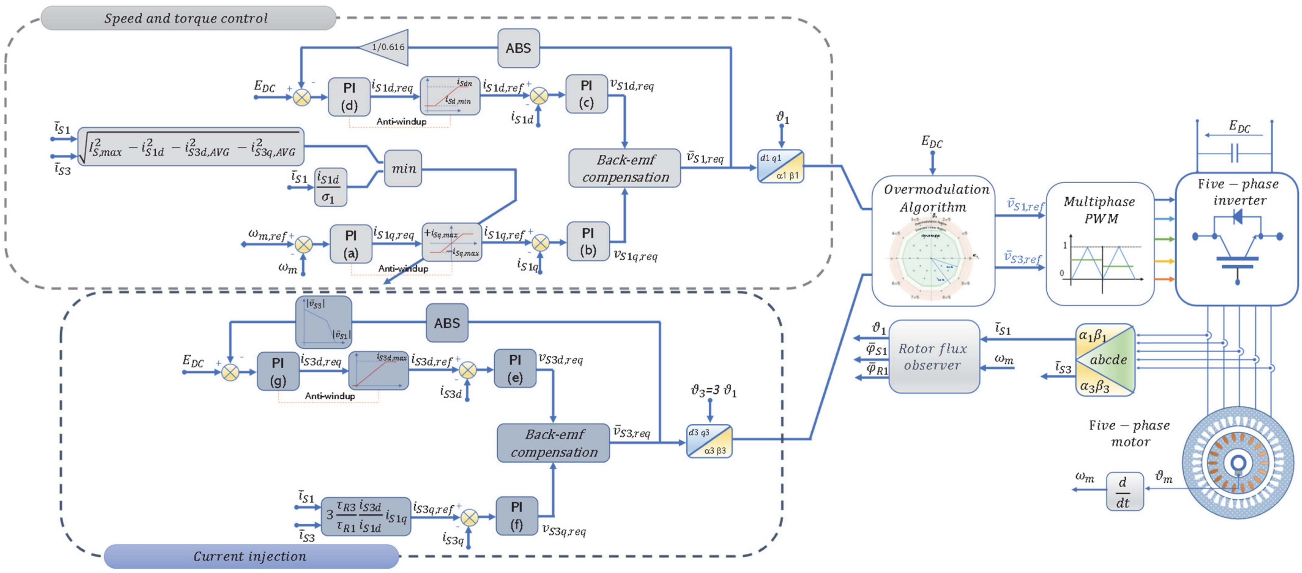

Fig. 2. Control scheme of the motor.

condition, the inverter overmodulation can significantly enhance the torque and power capability of the drive.

Although it is not possible to inject the current space vector $\bar{\imath}_{S3}$ to increase the torque density in the field-weakening region, voltage space vector $\bar{v}_{S3}$ can be used to extend the admissible range of $\bar{v}_{S1}$ resulting from (17), as shown in Fig. 1.

Given the desired value of $\bar{v}_{S1}$, the overmodulation algorithm proposed in [18] looks for a value of $\bar{v}_{S3}$ that satisfies (17). Since, in general, there are many solutions for $\bar{v}_{S3}$, the algorithm finds the one with the minimum magnitude of $\bar{m}_3$. As the current distortion is proportional to the value of $|\bar{m}_3|$, the solution selected in [18] makes it possible to minimize the harmonic distortion of the phase currents in a five-phase induction motor drive and reduce torque pulsation.

The reference value of $\bar{m}_3$ is split into two components, x_3 and y_3, respectively parallel and perpendicular to $\bar{A}_{3,HL}$.

$$\bar{m}_3 = \bar{A}_{3,HL}\left(x_3 + jy_3\right). \tag{24}$$

The quantities x_3 and y_3 are as follows:

$$x_3 = \frac{1 - \bar{m}_1 \cdot \bar{A}_{1,HL}}{\left|\bar{A}_{3,HL}\right|^2} \tag{25}$$

$$y_3 = \begin{cases} 0 & if \quad y_{HU}\, y_{LD} \leq 0 \\ y_{HU} & if \ |y_{HU}| \leq |y_{LD}| \\ y_{LD} & \quad otherwise \end{cases} \tag{26}$$

where:

$$y_{HU} = -\frac{\bar{m}_{1,ref} \cdot \bar{A}_{1,HU} + x_3\left(\bar{A}_{3,HL} \cdot \bar{A}_{3,HU}\right)}{\left(j\bar{A}_{3,HL} \cdot \bar{A}_{3,HU}\right)}$$
$$y_{LD} = -\frac{\bar{m}_{1,ref} \cdot \bar{A}_{1,LD} + x_3\left(\bar{A}_{3,HL} \cdot \bar{A}_{3,LD}\right)}{\left(j\bar{A}_{3,HL} \cdot \bar{A}_{3,LD}\right)}. \tag{27}$$

and $\bar{A}_{1,HU}$, $\bar{A}_{1,LD}$, $\bar{A}_{3,HU}$ and $\bar{A}_{3,LD}$ are defined similarly to (19).

As a result, (27) allows voltage space vector $\bar{v}_{S1}$ to reach a magnitude of $0.616\,E_{DC}$ and extend the linear modulation range by 17%.

Above this threshold, the inverter enters in the conventional overmodulation mode, and the desired value of $\bar{v}_{S1}$ cannot be obtained any more.

VI. Control Scheme

The block diagram of the control system for a five-phase machine is shown in Fig. 2. It combines the two control strategies illustrated in Sections III-V for high torque density in the linear and extended linear modulation regions. The control system can be separated in two main sections: the speed control loop and the current injection. It is based on a conventional rotor-flux oriented control scheme in the fundamental subspace where the stator and the rotor fluxes $\bar{\varphi}_{S1}$ and $\bar{\varphi}_{R1}$ are determined with a rotor flux observer based on (2), and the speed is calculated as the derivative of the rotor position measured with an incremental encoder.

The first section of the control scheme illustrates the speed control loop and the operation in extended linear modulation. The rotor speed is adjusted by the Proportional Integral (PI) regulator (a), which generates the reference current $i_{S1q,req}$. This signal, saturated between $\pm|i_{S1q,\max}|$, is tracked by regulator (b). The threshold $i_{S1q,\max}$ is calculated from the more restrictive constraint between the thermal limit of the machine and the breakdown torque expressed by (21) and (23), respectively. The current $i_{S1d,ref}$ is tracked using regulator (c), and the value of $i_{S1d,ref}$ is obtained from regulator (d), which manages the field-weakening operation of the machine until the extended linear modulation is reached.

When the magnitude of the voltage $\bar{v}_{S1,req}$ required by the current regulators becomes higher than the maximum voltage ($0.616\,E_{DC}$), regulator (d) decreases $i_{S1d,ref}$ to reduce the stator

TABLE I
PARAMETERS OF THE FIVE-PHASE MACHINE

$\omega_{m,rated} = 200\,rpm$	$p = 3$
$R_S = 1.7\,\Omega$	$R_{R1,3} = 2.03\,\Omega$
$L_{S1} = 410\,mH$	$L_{S3} = 68\,mH$
$L_{R1} = 399\,mH$	$L_{R3} = 65.8\,mH$
$M_1 = 362\,mH$	$M_3 = 35\,mH$

TABLE II
PARAMETERS OF THE FIVE-PHASE TWO-LEVEL INVERTER

$IGBT\ Imax = 10\,A, E_{DC} = 100\,V$
$Switching\ frequency = 5\,kHz, dead\ time = 1.6\,\mu s$
$DC - link\ capacitance\ 550\,\mu F$

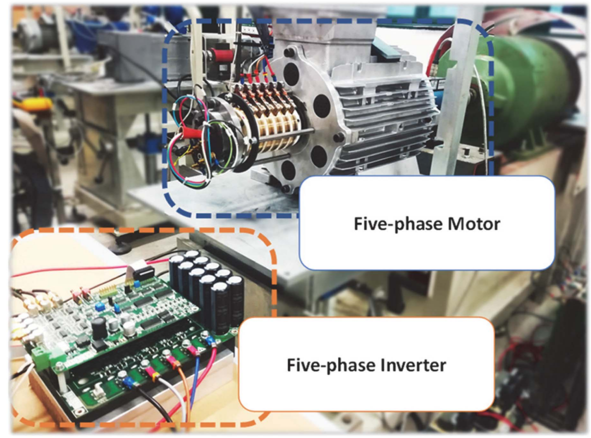

Fig. 3. Experimental set-up of the electric drive composed by a five-phase wound-rotor induction machine and a five-phase inverter.

flux and the back-EMF until the magnitude of $\bar{v}_{S1,req}$ fits in the extended linear modulation area.

Finally, the estimated $d_1 - q_1$ back-Electro Motive Forces (back-EMFs) are added to the output signals of the regulators (b) and (c) to improve the dynamic performance.

The second section of the block diagram manages the current injection in the low-speed region to perform the high-torque density. The q component of the current reference in the third subspace $i_{S3q,ref}$ is calculated by (13) and tracked using regulator (f). The current $i_{S3d,ref}$ is tracked by the regulator (e). Its value is obtained by saturating the output of the regulator (g) between 0 and $i_{S3d,\max}$. This quantity is the minimum between the value obtained from (12) and $i_{S1d,rated}/\sqrt{3}$, corresponding to an amplitude for the third harmonic of the air-gap magnetic field equal to 1/6 of the fundamental component [12].

Regulator (g) generates $i_{S3d,ref}$ considering the voltage constraints on the requested voltage vectors $\bar{v}_{S1,req}$ and $\bar{v}_{S3,req}$, expressed as follows:

$$\begin{cases} 2\left|\bar{v}_{S1,req}\right| \sin\left(\frac{\pi}{5}\right) + 2\left|\bar{v}_{S3,req}\right| \sin\left(\frac{2\pi}{5}\right) \leq E_{DC} \\ 2\left|\bar{v}_{S1,req}\right| \sin\left(\frac{2\pi}{5}\right) + 2\left|\bar{v}_{S3,req}\right| \sin\left(\frac{\pi}{5}\right) \leq E_{DC} \end{cases} \quad (28)$$

Given the desired voltage $\bar{v}_{S1,req}$ in the fundamental subspace, if the available voltage of the DC-link is not enough to inject the third harmonic component of the stator current according to (28), the refence current $i_{S3d,ref}$ is set to zero by regulator (g) to allow the motor to enter in the field weakening region. In this operating condition, the overmodulation block takes as input the value of $\bar{v}_{S1,ref}$ to calculate the minimum value of $\bar{v}_{S3,ref}$ by means of (24)–(27).

Finally, the gate signals are generated using a Pulse Width Modulation (PWM) strategy.

VII. EXPERIMENTAL RESULTS

The effectiveness of the proposed electric drive with high-torque density in the constant and reduced power region has been validated with a five-phase wound-rotor induction motor and a five-phase IGBT inverter. The experimental setup is shown in Fig. 3. The electric parameters of the motor and inverter are described in Tables I and II. The control scheme shown in Fig. 2 has been implemented using a rapid prototyping system based on dSPACE MicroLabBox.

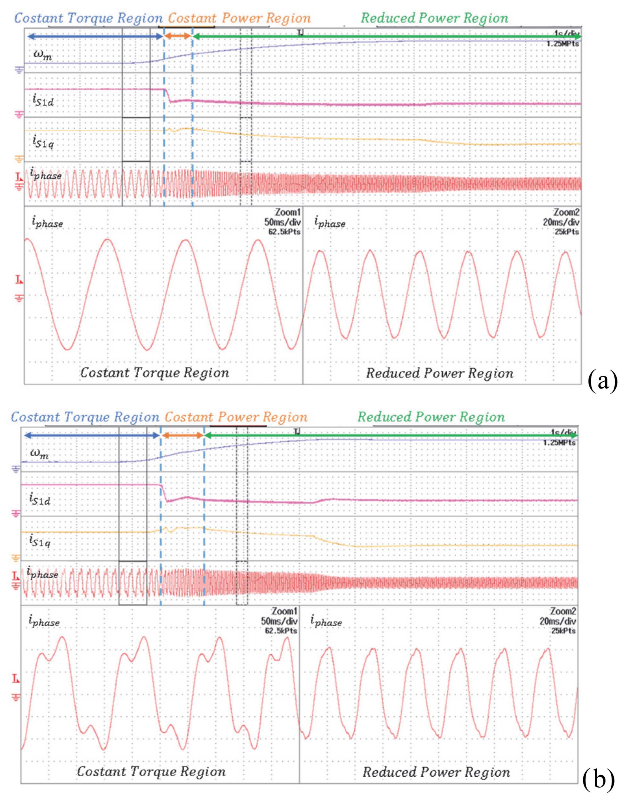

Fig. 4. Experimental result. Speed transient without third harmonic injection (a) and with third harmonic injection (b). ω_m (150 rpm/div), i_{S1d} (0.5 A/div), i_{S1q} (1 A/div), phase current (2 A/div).

Fig. 4(a) and (b) show the speed transient of the electric drive up to four times the base speed when the control of subspace $d_3 - q_3$ is respectively disabled and enabled.

In Fig. 4(a), when the current and voltage injection in subspace $d_3 - q_3$ is not used, the motor passes through the constant-torque region, the constant-power region and finally reaches the decreasing-power region. In all the operating conditions, the stator current has a sinusoidal waveform. As expected, the

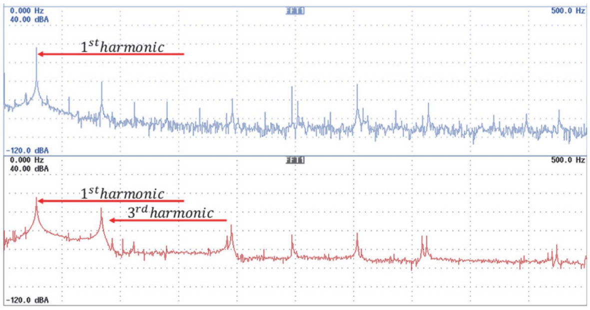

Fig. 5. Experimental result. Comparison of current spectra at a steady state in the constant torque region without third harmonic injection (blue) and with third harmonic injection (red).

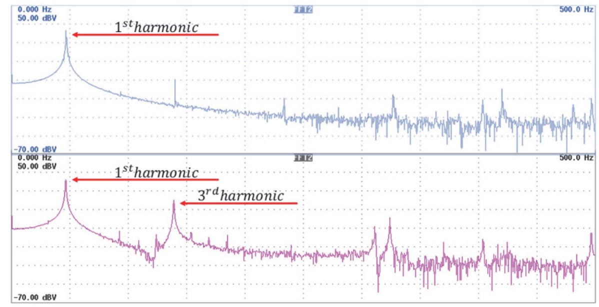

Fig. 6. Experimental result. Comparison of line voltage spectra at a steady state in the reduced power region without inverter overmodulation (blue) and with inverter overmodulation (magenta).

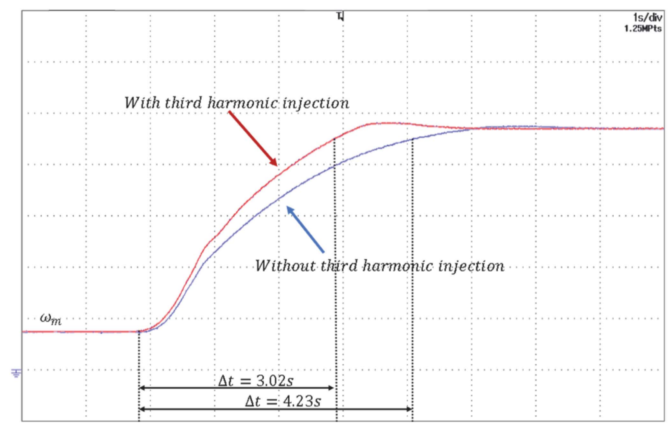

Fig. 7. Experimental result. Dynamic response during a rotor speed transient with and without the third harmonic injection. Mechanical speed ω_m (150 rpm/div).

amplitude of the phase current is constant and equal to the maximum value in the first and second region. Then, it decreases in the third region.

It is worth noting that the speed range of the constant-power region is very limited due to the specific parameters of the machine under test.

Fig. 4(b) illustrates the behavior of the drive in the same condition as Fig. 4(a) when the harmonic injection in subspace $d_3 - q_3$ is enabled. In the constant-torque region, the injection of the current $\bar{\imath}_{S3,\ ref}$ distorts the phase currents but keeps the overall RMS value constant.

When the DC-link voltage is insufficient to inject the desired current $\bar{\imath}_{S3,\ ref}$, the setpoint is progressively set to zero by the control system. From that moment on, the inverter operates in the extended linear region, where $\bar{v}_{S3,ref}$ is used to widen the admissible range of $\bar{v}_{S1,ref}$.

Therefore, the phase current shows a slight distortion even in the high-speed region. The amplitude of the current ripple is minimal due to the high value of the electrical time constant, which is typical in induction motors.

As expected in the theoretical analysis, the motor torque increases by about 7% in the constant-torque region. The maximum motor torque in the field weakening region depends on the square of the available voltage $V_{S,\max}$. Therefore, an increase in $V_{S,\max}$, achieved by widening the linear modulation range, significantly increases the torque capability.

Fig. 5 reports the spectra of the phase current up to 500 Hz when the motor operates at a steady state in the constant torque region, with and without the third harmonic injection. As shown, if the harmonic injection is enabled to increase the torque density and improve the dynamic response, the third-harmonic component of the current rises by about 20 dB.

Fig. 6 shows the spectra of the phase voltage in a steady state when the machine operates in the flux weakening region with and without inverter overmodulation. In the case of overmodulation, a third harmonic component, which is 20 dB higher, is generated in the stator voltage to enhance the power capability.

Fig. 7 compares the duration of the speed transients due to the application of a step reference, with and without third harmonic injection, to evaluate the effect of the increased torque of the machine. The purpose of this test is to emphasize that careful use of the additional degrees of freedom in a multiphase system can lead to a notable improvement in the performance of the motor. During the tests, the speed is regulated by the closed-loop control scheme shown in Fig. 2, which ensures zero error in steady-state conditions independently of the third harmonic current injection. However, the third-harmonic injection allows the motor to generate higher torque values below the base speed. Consequently, the slope of the corresponding speed curve is visibly higher during the entire transient. Comparing the two dynamic responses, it can be concluded that injecting the third harmonic reduces the rise time (time to 95% of the steady-state speed) by approximately 28.5%. As a result, the dynamic response of the motor can be substantially enhanced by the high-torque density control strategy.

Fig. 8 shows the torque and output power of the motor. The data collect the maximum torque generated by the machine at different operating speeds under steady-state conditions while using the proposed control scheme with and without third harmonic injection. The proposed solution offers a remarkable advantage in the high-speed region, where the slightest increase in the available voltage leads to a substantial boost in mechanical power. In scenarios where speed and power are the most important factors, such as automotive traction, this increase in performance can be a breakthrough.

Fig. 9 shows the ratio of the torque values produced with and without third harmonic injection in steady state conditions.

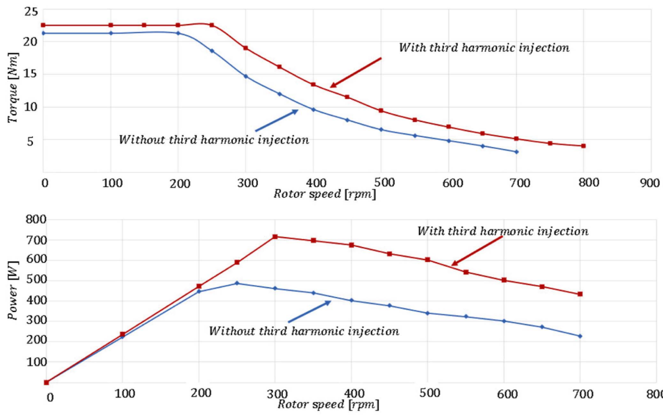

Fig. 8. Experimental result. Mechanical torque and power with and without the third-harmonic injection in steady-state conditions.

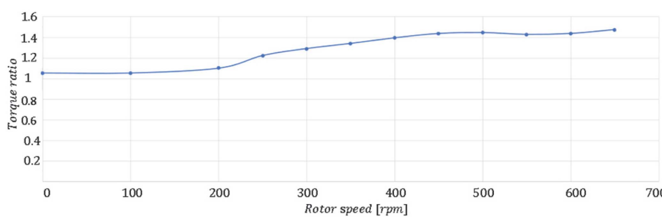

Fig. 9. Experimental result. Ratio of the steady-state motor torques with and without third-harmonic injection.

As expected, injecting a third harmonic can increase the torque by over 40% with a significant advantage when the machine operates in the field-weakening region.

VIII. Conclusion

This paper investigates the use of the degrees of freedom in a five-phase induction motor to improve drive performance over the whole speed range.

At low speed the developed electric drive generates a third-harmonic current into the $d_3 - q_3$ subspace. This approach improves the magnetic field distribution in the air gap and prevents the magnetic saturation of the machine. Injecting the third harmonic current can thereby increase the output torque of the machine.

In the field-weakening region, where the available inverter voltage is constrained, the control scheme applies a voltage space vector different from zero in the $d_3 - q_3$ subspace, which extends the linear modulation range of the fundamental voltage in the $d_1 - q_1$ subspace and enhances the machine performance.

The control scheme considers both voltage and current constraints to improve static and dynamic performance, and it guarantees that the motor does not surpass its thermal limit.

The proposed control scheme offers significant advantages, particularly at high speed. The theoretical analysis shows that the output power of the motor can increase by over 40% at high speeds, due to the square relationship between torque and voltage. This significant improvement in performance can considerably increase the promptness of the machine.

The experimental tests confirm the feasibility and the effectiveness of the proposed solution based on harmonic current and voltage injection. This result demonstrates that the proposed approach is not only effective but also practical in real-world applications. The performance of the machine is significantly improved throughout its speed range, making it suitable for various industrial solutions.

References

[1] E. Levi, "Advances in converter control and innovative exploitation of additional degrees of freedom for multiphase machines," *IEEE Trans. Ind. Electron.*, vol. 63, no. 1, pp. 433–448, Jan. 2016.

[2] F. Barrero and M. J. Duran, "Recent advances in the design, modeling, and control of multiphase machines—Part I," *IEEE Trans. Ind. Electron.*, vol. 63, no. 1, pp. 449–458, Jan. 2016.

[3] L. Parsa and H. A. Toliyat, "Fault-tolerant interior-permanent-magnet machines for hybrid electric vehicle applications," *IEEE Trans. Veh. Technol.*, vol. 56, no. 4, pp. 1546–1552, Jul. 2007.

[4] H. S. Che, M. J. Duran, E. Levi, M. Jones, W.-P. Hew, and N. A. Rahim, "Postfault operation of an asymmetrical six-phase induction machine with single and two isolated neutral points," *IEEE Trans. Power Electron.*, vol. 29, no. 10, pp. 5406–5416, Oct. 2014.

[5] R. Kianinezhad, B. Nahid-Mobarakeh, L. Baghli, F. Betin, and G.-A. Capolino, "Modeling and control of six-phase symmetrical induction machine under fault condition due to open phases," *IEEE Trans. Ind. Electron.*, vol. 55, no. 5, pp. 1966–1977, May 2008.

[6] A. Tani, M. Mengoni, L. Zarri, G. Serra, and D. Casadei, "Control of multiphase induction motors with an odd number of phases under open-circuit phase faults," *IEEE Trans. Power Electron.*, vol. 27, no. 2, pp. 565–577, Feb. 2012.

[7] E. Levi, M. Jones, S. N. Vukosavic, and H. A. Toliyat, "A novel concept of a multiphase, multimotor vector controlled drive system supplied from a single voltage source inverter," *IEEE Trans. Power Electron.*, vol. 19, no. 2, pp. 320–335, Mar. 2004.

[8] H. S. Che, E. Levi, M. Jones, M. J. Duran, W. -P. Hew, and N. A. Rahim, "Operation of a six-phase induction machine using series-connected machine-side converters," *IEEE Trans. Ind. Electron.*, vol. 61, no. 1, pp. 164–176, Jan. 2014.

[9] K. K. Mohapatra, R. S. Kanchan, M. R. Baiju, P. N. Tekwani, and K. Gopakumar, "Independent field-oriented control of two split-phase induction motors from a single six-phase inverter," *IEEE Trans. Ind. Electron.*, vol. 52, no. 5, pp. 1372–1382, Oct. 2005.

[10] A. S. Abdel-Khalik, M. I. Masoud, S. Ahmed, and A. M. Massoud, "Effect of current harmonic injection on constant rotor volume multiphase induction machine stators: A comparative study," *IEEE Trans. Ind. Appl.*, vol. 48, no. 6, pp. 2002–2013, Nov./Dec. 2012.

[11] A. S. Abdel-Khalik, M. I. Masoud, and B. W. Williams, "Improved flux pattern with third harmonic injection for multiphase induction machines," *IEEE Trans. Power Electron.*, vol. 27, no. 3, pp. 1563–1578, Mar. 2012.

[12] M. Mengoni, L. Zarri, A. Tani, L. Parsa, G. Serra, and D. Casadei, "High-torque-density control of multiphase induction motor drives operating over a wide speed range," *IEEE Trans. Ind. Electron.*, vol. 62, no. 2, pp. 814–825, Feb. 2015.

[13] Y. Wang, J. Yang, G. Yang, S. Li, and R. Deng, "Harmonic currents injection strategy with optimal air gap flux distribution for multiphase induction machine," *IEEE Trans. Power Electron.*, vol. 36, no. 1, pp. 1054–1064, Jan. 2021.

[14] E. Libbos, E. Krause, A. Banerjee, and P. T. Krein, "Winding layout considerations for variable-pole induction motors in electric vehicles," *IEEE Trans. Transp. Electrific.*, vol. 9, no. 4, pp. 5214–5225, Dec. 2023.

[15] V. T. Buyukdegirmenci, A. M. Bazzi, and P. T. Krein, "Evaluation of induction and permanent-magnet synchronous machines using drive-cycle energy and loss minimization in traction applications," *IEEE Trans. Ind. Appl.*, vol. 50, no. 1, pp. 395–403, Jan./Feb. 2014.

[16] A. Salem and M. Narimani, "A review on multiphase drives for automotive traction applications," *IEEE Trans. Transp. Electrific.*, vol. 5, no. 4, pp. 1329–1348, Dec. 2019.

[17] A. Salem and M. Narimani, "New powertrain configurations based on six-phase current-source inverters for heavy-duty electric vehicles," *IEEE Access*, vol. 10, pp. 87563–87576, 2022.

[18] L. Vancini, M. Mengoni, G. Rizzoli, G. Sala, L. Zarri, and A. Tani, "Carrier-based PWM overmodulation strategies for five-phase inverters," *IEEE Trans. Power Electron.*, vol. 36, no. 6, pp. 6988–6999, Jun. 2021.

[19] L. Vancini, M. Mengoni, G. Rizzoli, L. Zarri, and A. Tani, "Control of a five-phase induction motor drive with high-torque density and voltage overmodulation," in *Proc. IEEE Energy Convers. Congr. Expo.*, 2022, pp. 1–6.

[20] J. Malvar et al., "Graphical diagram for subspace and sequence identification of time harmonics in symmetrical multiphase machines," *IEEE Trans. Ind. Electron.*, vol. 61, no. 1, pp. 29–42, Jan. 2014.

[21] A. G. Yepes and J. Doval-Gandoy, "Overmodulation method with adaptive *x-y* current limitation for five-phase induction motor drives," *IEEE Trans. Ind. Electron.*, vol. 69, no. 3, pp. 2240–2251, Mar. 2022.

Luca Vancini (Member, IEEE) received the M.Sc. and Ph.D. degrees in electrical engineering from the University of Bologna, Bologna, Italy, in 2018 and 2022, respectively. He is currently a Research Fellow with the Department of Electrical, Electronic and Information Engineering "G. Marconi", University of Bologna. His research interests include power electronics, control of multiphase converters, and diagnostic techniques for multiphase machines.

Michele Mengoni (Member, IEEE) received the M.Sc. (withHons.) and Ph.D. degrees in electrical engineering from the University of Bologna, Bologna, Italy, in 2006 and 2010, respectively. He is currently an Associate Professor with the Department of Electrical, Electronic and Information Engineering "G. Marconi", University of Bologna. His research interests include design, analysis, and control of three phase electric machines, multiphase drives, and AC/AC matrix converters. He is also an Associate Editor for IEEE Transaction on Industrial Electronics.

Gabriele Rizzoli received the M.Sc. and Ph.D. degrees (with Hons.) in electrical engineering from the University of Bologna, Bologna, Italy, in 2012 and 2016, respectively. He is currently an Assistant Professor with the Department of Electrical, Electronic and Information Engineering "G. Marconi", University of Bologna. His research interests include the design of electrical machines, the development and control of high-efficient power converters for automotive and renewable energy applications.

Luca Zarri (Senior Member, IEEE) received the M.Sc. and Ph.D. degrees in electrical engineering from the University of Bologna, Bologna, Italy, in 1998 and 2007, respectively. He is currently a Full Professor of power electronics, electrical machines and drives with the Department of Electrical, Electronic, and Information Engineering "Guglielmo Marconi", University of Bologna. He has authored or coauthored more than 190 scientific papers. His research interests include the control of power converters and electric drives. He is a senior member of the *IEEE Industry Applications*, IEEE Power Electronics, and IEEE Industrial Electronics Societies. He was the Chair of the IEEE IAS Industrial Drives Committee during2022–2023. He is also the Vice Chair of the Industrial Power System Department.

Angelo Tani received the M. Sc. degree in electrical engineering (with Hons.) from the University of Bologna, Bologna, Italy, in 1988. He is currently a Full Professor of power electronics, electrical machines and drives with the Department of Electrical, Electronic and Information Engineering "Guglielmo Marconi", University of Bologna. He has authored more than 200 papers published in technical journals and conference proceedings. His research interests include modeling, control, and fault diagnosis of multiphase electric machines.